Supporting Information

Hao et al. 10.1073/pnas.1100432108

SI Materials and Methods

Construction of Strains and Plasmids. We constructed a series of reporter system to quantify RyhB–*sodB* interaction using a strategy introduced earlier by Levine et al. (1). Experiments were performed in ZZS00 cells derived from *Escherichia coli* K-12 BW25113 with chromosomal *ryhB* deleted and a cassette *spr-lacI-tetR* inserted at the *attB* site of the chromosome to provide constitutive expression of *lacI* and *tetR*. Then two types of plasmids, one carrying *ryhB* or its mutant (pZA31R#, pZA31RH#, pZA31RC#) and the other carrying the translational fusion of *sodB* (or its mutant) with the reporter gene *gfpmut3b* (pZE12SC#), were transformed into ZZS00 to generate three series of mutant strains ZZS00-R#, ZZS00-C#, and ZZS00-H#, as listed in Table S1. The strain containing plasmids harboring wild-type RyhB and wild-type *sodB* (pZA31R and pZE12S, respectively), called ZZS00-W here, is the same as ZZS23 used in ref. 1.

The small RNA (sRNA)-source plasmid was derived from the pZA31-luc*NB* plasmid, which contained p15A replication *ori* and was marked by chloramphenicol-resistance (2). The *luc* gene was driven by the synthetic $P_{LTet\text{-}O1}$ promoter inducible by anhydrotetracycline (aTc). The wild-type *ryhB* gene was cloned directly from *E. coli* K-12 and ligated into the NdeI/BamHI sites to replace the *luc* gene, yielding the wild-type RyhB-source plasmid (pZA31R).

The mRNA-source plasmid was derived from the pZE12G plasmid, which contained colEI replication *ori* and was marked by ampicillin resistance (2). The *gfpmut3b* structural gene on pZE12G was driven by the synthetic $P_{Llac\text{-}O1}$ promoter (2) inducible by isopropyl β-D-thiogalactoside (IPTG). The 5′ UTR from the control region of *sodB* (crsodB, from −1 to +88 relative to the transcriptional start site and including the first 11 codons of *sodB*) was cloned into the EcoRI and KpnI sites, yielding the wild-type *sodB* source plasmid (pZE12S).

The *sodB* mutants constituting the pZE12SC# series were amplified with two rounds of PCR. The first round of amplification was done with primer "sc-f" and "sc#-r" (#: 1–15), with wild-type *sodB* as template. Primers "s0-f" and "s0-r" were used in the second round of PCR using the first-round PCR products as templates. The products from the second PCR were digested with restriction enzymes EcoRI and KpnI, then inserted into the same sites of pZE12G, yielding various *sodB* mutants plasmids (pZE12SC#). Plasmids and primers used in this study are listed in Table S2 and Table S3, respectively.

The *ryhB* mutants constituting the pZA31RC# series were also amplified with two rounds of PCR using the above procedure. The primers used in the first round were "rc#-f" (#: 1–15) and "rc-r." We did not add template into the reaction solution of the first round because there were 17 complementary bases at the 3′ end of the two primers, so the templates were obtained during the amplification. Primers "r0-f" and "r0-r" were used in the second round using the products from the first round as templates. The products from the second PCR were digested using restriction enzyme NdeI and BamHI, then were inserted into the sites of pZA31-*lucNB*, yielding various *ryhB* mutant plasmids (pZA31RC#).

The truncated *ryhB* (*ryhBt*) was constructed by annealing oligonucleotides directly. The "sensechain"(AAACATATGAAGCACGACATTGCTCACATTGCTTAGCCAGCCGGGTGCTGGCTTTTTTTTTGGATCCTTT, with NdeI sites and BamHI sites underlined) and "antisensechain"(AAAGGATCCAAAAAAAAAGCCAGCACCCGGCTGGCTAAGCAATGTGAGCAATGTCGTGCTTCATATGTTT, with BamHI sites and NdeI sites underlined) were resuspended at the same molar concentration of 2 OD/100 μL in "annealing buffer" [10 mM Tris (pH 8.0), 50 mM NaCl, 1 mM EDTA]. The solutions were mixed with equal volumes in a 1.5-mL tube to be placed at 94 °C for 5 min, then the tube was slowly cooled down to room temperature (below 25 °C, for half an hour). After being stored at 4 °C for half an hour, the products were digested using NdeI and BamHI before insertion into digested pZA31-*luc*NB.

The DNA fragments of the mutant *ryhB* in the R- and H-series were synthesized using an ABI 391 DNA synthesizer following a doped oligosynthesis procedure to generate random substitution. We replaced the four reservoirs each containing a single phosphoramidite with those containing combinations of phosphoramidite (the ratio of the four different phosphoramidite was 70:10:10:10 for the H-mutants to simulate a 30% substitution frequency, and was 90:3.3:3.3:3.3 for the R-mutants to simulate a 10% substitution frequency) (3). The synthesized fragments were amplified using primers "r0-f" and "r0-r" and digested using NdeI and BamHI. They were inserted into the same sites of pZA31-*lucNB* and then were transferred into ZZS20. Then the GFP expression of these strains was characterized upon induction with 1 mM IPTG and 0 or 10 ng/mL aTc. Most of the R-mutants lost their ability to repress sodB-GFP expression, whereas the H-mutants were still able to repress to various degrees. Table S4 contains sequences for all of the R-mutants that had more than twofold repression as well as a number of randomly selected ineffective ones. For the H-mutants, all of the 19 strains tested were kept. All of the characterized strains were verified by sequencing (using primers "ZA31-f" and "ZA31-rn").

To construct a background strain ZZS00-NULL (measured as negative control), we deleted the $P_{Llac\text{-}O1}$ promoter of pZE12G to yield pNULL plasmid and then transformed both pNULL and pZA31-*lucNB* to cell ZZS00.

To determine the effects of single-copy *ryhB* or its derivatives on expression of its targets, the $P_{Ltet\text{-}O1}$-driving *ryhB* and *ryhBt* as present in respective pZA31R plasmids (Table S2) were moved to the *ryhB* locus of the ZZS00 chromosome using the method described in Klumpp et al. (4). Briefly, to make the chromosomal $P_{Ltet\text{-}O1}$ driving *ryhB*, the km:*rrnB*T:$P_{Ltet\text{-}O1}$ construct present in pKDT-*rrnB*T:$P_{Ltet\text{-}O1}$ (4) was amplified using primers PtetryhB1-P1 and PtetryhB1-P2 (Table S3). The PtetryhB1-P1 contains a 50-bp region that is homologous to the upstream region of the *ryhB* promoter, whereas PtetryhB2-P2 contains a 50-bp region that is reverse complemented to the first 50-bp region of the *ryhB* gene. The PCR products were gel purified and then electroporated into ZZS00 cells expressing the λ–Red recombinase. The cells were incubated with shaking at 37 °C for 1 h and then applied onto LB + Km agar plates. The plates were incubated at 30 °C overnight. The Km resistant colonies were verified for the substitution of the native *ryhB* promoter by colony PCR and subsequently by sequencing. The resultant strain was named ZZS0R. To make chromosomal $P_{Ltet\text{-}O1}$ driving *ryhBt*, a long reverse primer (PtetryhBt2-P2) was synthesized, which carries the entire *ryhBt* and the 24 nucleotides immediately downstream of the 9-T tract of the *ryhB* gene (Table S3). The km:*rrnB*T:$P_{Ltet\text{-}O1}$-*ryhBt* was amplified from pKDT-*rrnB*T:$P_{Ltet\text{-}O1}$ using primers PtetryhB1-P1 and PtetryhBt2-P2. The PCR products were integrated into the chromosome of ZZS00 cells as described above. The resultant strain, in which K_m:*rrnB*T:$P_{Ltet\text{-}O1}$-*ryhBt* is substituted for *ryhB* and its promoter, is named ZZS0T. The *hfq* mutation was transferred by P1 transduction to ZZS0R and ZZS0T, yielding strains ZZS0Rq and ZZS0Tq, respectively. All

the plasmid and chromosomal constructs were verified by PCR and DNA sequencing.

Medium, Growth, and Measurements. The ZZS00 cells carrying the appropriate plasmids were grown with shaking to midlog phase ($OD_{600} \approx 0.5$) in M63 minimal media at 37 °C with 0.5% glucose and standard concentrations of the appropriate antibiotics. The cells were diluted (1:250) to fresh media and shaken overnight. The cultures were diluted again into fresh M63 media (OD_{600} = 0.002) containing the appropriate antibiotics and carbon source, as well as varying amounts of the inducers (aTc and IPTG) in wells of 48-well plates. The plates were incubated with shaking at 37 °C and examined for OD_{600} and fluorescence measurements every 0.5–1 h for up to 10 h (until a final OD_{600} of 0.2) using a Wallac Victor3 1420 multilabel counter (PerkinElmer Life Sciences). Each measurement was repeated three times, and the data were analyzed similarly as in ref. 1.

Quantitative Real-Time PCR. For quantitative real-time PCR, strains were cultured in liquid LB with appropriate antibiotics for 6 h. The cultures were diluted at least 1,000-fold in M63 plus 0.5% glucose and appropriate concentrations of antibiotics (Cm, Ap) and inducer (10 ng/mL aTc). After ≈13 h of growth, the cultures were inoculated at OD_{600} of 0.025 to identical fresh media. When OD_{600} reached ≈0.5, two samples of 0.6 mL of culture were collected and treated by RNAprotect Bacteria Reagent (Qiagen; catalog no. 76506) to inactivate RNase activities before RNA preparation. Total RNA was prepared using either a RNeasy Mini Kit (Qiagen; catalog no. 74104) or a miRNeasy Mini Kit (Qiagen; catalog no. 217004). The RNA samples were treated with Turbo DNA-free DNase (Ambion; catalog no. 1907) to remove any residual genomic DNA. Typically, 50 ng total RNA was used for cDNA synthesis and subsequent real-time PCR in the same tube using iScriptTM One-Step RT-PCR Kit with SYBR Green (Bio-Rad; catalog no. 172-8892). *rrsB*, encoding 16S RNA, was included as an internal control; in these reactions 0.5 ng total RNA was used because of the extreme abundance of *rrsB*. In some cases serial dilutions of the RNA sample were made to obtain more accurate quantification by correcting for imperfect reaction efficiency. In these cases, starting RNA was serially twofold (eight consecutive dilutions) or fivefold (five consecutive dilutions) diluted. In all cases, real-time PCR was carried out in a Bio-Rad iQ5 Multicolor Real-Time PCR Detection System. Primers used in quantitative real-time PCR are listed in Table S3.

For the data analyses, for each target the mRNA level in the hfq^+ strain carrying the chromosomal *ryhBt* and growing with no aTc was arbitrarily set to be 1. The mRNA levels for the same target in hfq^+ or hfq^- strains and growing with or without aTc were shown relative to 1.

For the dilution series analysis, a line was fit to the plot of relative initial RNA amount vs. C_t, the cycle threshold, for both the target and reference genes. The slope of this line was used to estimate the efficiency of PCR amplification for each amplicon. The ratio of target to reference gene was then computed for each point in the dilution series using the corrected efficiencies, and the average of those values is reported as the expression level of the RNA.

Energy Calculation and RNA Structure. We calculated the ensemble free energy of every RNA/RNA-duplex structure with or without constraint using the Vienna RNA Package (http://www.tbi.univie.ac.at/RNA/). E_{RyhB}, E_{sodB}, and E_{duplex}, which denote the self-binding free energy for RyhB, self-binding free energy for the *sodB* control region, and the free energy of RyhB-*sodB* duplex, respectively, were obtained without constraint. For wild-type *sodB* and its mutants, we forced both the interaction core region (52–60 in Fig. S1) and Hfq-binding site (29–44 in Fig. S1) single stranded, and calculated the difference (E^*_{sodB}) between the free energy of the constrained and unconstrained structures. ΔE_{linker} for wild-type RyhB and its mutants were calculated as the difference between the free energy of unconstrained structure and the structure constrained Hfq-binding sites (positions 57–68 in Fig. S1) single stranded. The minimal free energy structures were predicted by the RNAstructure software (http://rna.urmc.rochester.edu/RNAstructure.html).

Data Analysis. ***GFP expression.*** The data were obtained from different repeats for each combination of strain and inducers. Following the analysis of Levine et al. (1), we first obtained the cell doubling rate [μ, the slope of a linear fit of $\log_2(OD_{600})$ vs. time] for each strain and condition, yielding a doubling time of ≈1.2 h for most strains. Next, for all of the time points, we plotted the average fluorescence vs. average OD_{600} (the background fluorescence production rate, which was obtained in the same way from the negative control strain ZZS00-NULL, had been removed) and extracted the slope (f). Taking account of the maturation kinetics of GFPmut3 (maturation half-life Γ ≈30 min), we computed the raw fluorescence production rate per growing cell $f\mu(1+\mu\Gamma)$ as GFP expression (5).

Global fit. To fit the experimental data with the steady-state solution (Eq. **1**, main text), we assumed that the GFP expression defined above is proportional to the steady-state mRNA level m (i.e., GFP expression = $b{\cdot}m$, where b reflects the rate of GFP translation and maturation). We first measured the expression of wild-type sodB-GFP under various concentration of IPTG (0.04–1 mM) and no aTc, yielding a relationship of every unit (1 nM/min) of α_m amounts to GFP expression of ≈116,000RFU/OD/h.

$$\begin{aligned}\text{GFP expression} &= b \cdot m = f(\alpha_m, \alpha_s, \lambda) \\ &= \frac{1}{2\beta_m}[(\alpha_m - \alpha_s - \lambda) + \sqrt{(\alpha_m - \alpha_s - \lambda)^2 + 4\lambda\alpha_m}]. \end{aligned} \quad \textbf{[S1]}$$

In the previous work (1), the wild-type RyhB–*sodB* interaction was discussed under different RyhB expression level, therefore α_s took different values for different experiments. As the parameter λ, which indicated the interaction strength between wild-type RyhB and *sodB*, was independent of RyhB activity, it was chosen as a global parameter in their work. In our mutation study, λ was chosen to indicate the interaction strength of different RyhB-*sodB* pairs. To find the difference of interaction strength among strains, we fitted the expression data to Eq. **1** (main text) using standard Levenberg-Marquardt algorithm. The best-fit parameters including a single parameter α_s shared for all of the seven strains (ZZS00-W, ZZS00-C3, ZZS00-C8, ZZS00-C9, ZZS00-C10, ZZS00-C11, and ZZS00-C15) and strain-dependent λs were obtained at confidence level of 95%.

1. Levine E, Zhang Z, Kuhlman T, Hwa T (2007) Quantitative characteristics of gene regulation by small RNA. *PLoS Biol* 5:e229.
2. Lutz R, Bujard H (1997) Independent and tight regulation of transcriptional units in *Escherichia coli* via the LacR/O, the TetR/O and AraC/I1-I2 regulatory elements. *Nucleic Acids Res* 25:1203–1210.
3. ABI (2002) *PCR-Mate EP Model 391 DNA Synthesizer: User's Manual* (Applied Biosystems, Foster City, CA).
4. Klumpp S, Zhang Z, Hwa T (2009) Growth rate-dependent global effects on gene expression in bacteria. *Cell* 139:1366–1375.
5. Leveau JH, Lindow SE (2001) Predictive and interpretive simulation of green fluorescent protein expression in reporter bacteria. *J Bacteriol* 183:6752–6762.

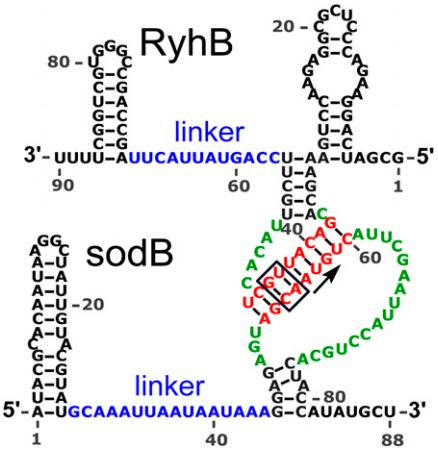

Fig. S1. RyhB–sodB interaction. A schematic representation of the experimentally derived interaction map between the sRNA RyhB (*Upper*) and one of its strongest targets, the mRNA of sodB (*Lower*) (1). The nucleotides in red represent the core complementarity region, which includes the start codon (AUG) of sodB (indicated by the arrow). Nonbinding nucleotides flanking the core are shown in green. The AU-rich regions (indicated in blue) bind to Hfq. Three mutant series were studied: the R-mutants contained various mutations in the interaction region of RyhB (R#), from nucleotide 32 through 56. The C-mutants include all 15 combinations of complementary point mutations of the two base pairs indicated by the black box (positions 54, 55 of sodB and 43, 44 of RyhB). The H-mutants include various mutations in the Hfq-binding region of RyhB (positions 57–68). All sequences are given in Tables S4, S5, and S6.

1. Geissmann TA, Touati D (2004) Hfq, a new chaperoning role: Binding to messenger RNA determines access for small RNA regulator. *EMBO J* 23:396–405.

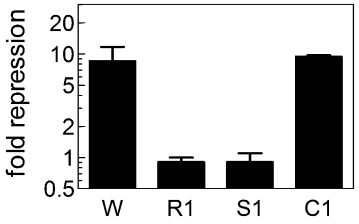

Fig. S2. Effect of compensatory mutations on *sodB* silencing by RyhB. Wild-type RyhB showed strong silencing ability on wild-type *sodB* (fold-repression ≈8.5). Single point substitution in RyhB (plasmid pZA31RC1, with U substituted by A at position 43 of the transcribed ryhB sequence) or *sodB* (plasmid pZE12SC1, with A substituted by U at position 55 of the transcribed sodB sequence) alone abolished repression (fold-repression ≈0.9 for both strain ZZS00-R1 and ZZS00-S1), whereas compensatory mutations restored repression (fold-repression ≈9 for strain ZZS00-C1 containing both pZA31RC1 and pZE12SC1) to a level comparable to that of the wild-type strain ZZS00-W).

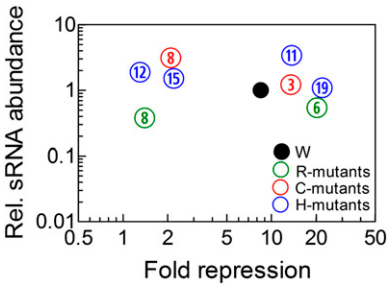

Fig. S3. Expression levels of plasmid-encoded *ryhB* mutants. The abundances of the wild-type RyhB (strain ZZS00-W, filled black circle) and selected mutants from the R-, C-, and H-series (green, red, and blue circles, respectively) in the absence of sodB-GFP expression were determined by quantitative real-time PCR in strains induced with 10 ng/mL aTc (*SI Materials and Methods*). The encircled number indicates the mutant number of a particular series indicated by the color (e.g., "11" in blue refers to the mutant H11). The *y* axis shows the RNA abundance of a mutant relative to the wild-type RyhB level in ZZS00-W, with the numerical values listed in Table S8. The *x* axis shows the degree of repression exerted by this mutant on sodB-GFP expression (data from Table S7). No correlation is seen between sRNA abundance and fold-repression. Note that the abundances of the RyhB mutants were mostly within two- to threefold of that of the wild type. This difference is not significant because the variation in the repeatability of these results is no less than twofold. One strain characterized (R11) did not give any RNA reading and was deemed not expressed.

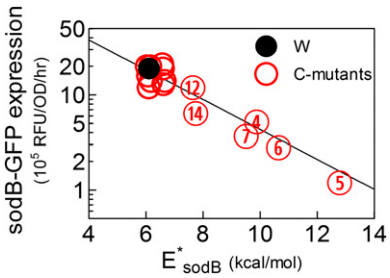

Fig. S4. Correlations between E*sodB and sodB-GFP expression of C-mutants in the absence of RyhB expression. We forced both the interaction core region (52–60 in Fig. S1) and Hfq-binding site (29–44 in Fig. S1) of sodB mutants single stranded, and calculated the difference (E*sodB) between the free energy of the constrained and unconstrained structures (*SI Materials and Methods*). The results are listed in Table S10. A clear exponential correlation is seen between E*sodB and sodB-GFP expression in the absence of RyhB expression, suggesting that altered sodB mRNA secondary structure in the vicinity of the start codon was responsible for the reduced expression levels observed. The black line shows the form $e^{-\beta E^*_{sodB}}$ with $\beta^{-1} \approx 2.78$ kcal/mol. The thermodynamic model has been used in explaining the control of translation by local secondary structure of mRNA in the vicinity of the start codon (1, 2), and a similar exponential relationship was detected in designing synthetic ribosome binding sites to control the expression of the red fluorescent protein (2).

1. de Smit MH, van Duin J (1994) Control of translation by mRNA secondary structure in *Escherichia coli*. A quantitative analysis of literature data. *J Mol Biol* 244:144–150.
2. Salis HM, Mirsky EA, Voigt CA (2009) Automated design of synthetic ribosome binding sites to control protein expression. *Nat Biotechnol* 27:946–950.

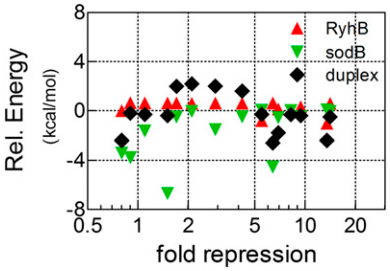

Fig. S5. Lack of correlation between fold-repression and the other energy scales of the system. Namely, the self-binding energies of RyhB (red) and *cr-sodB* (control region of *sodB* mRNA, green), and the RyhB-*sodB* duplex formation energy (black). The energy values here are the relative ones compared with the respective values for the wild type.

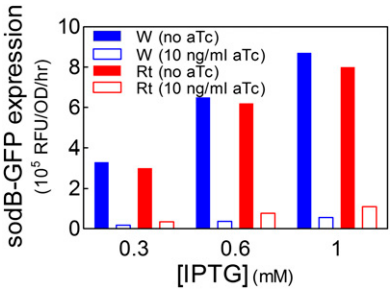

Fig. S6. sodB-GFP expressions in strains ZZS00-Rt and ZZS00-W with and without the inducer aTc. Red and blue bars refer to effects by RyhBt and the wild-type RyhB, respectively; open and solid bars refer to results with and without aTc, respectively.

Table S1. Bacterial strains used in this study

Strain/strain series	Genotype/plasmid	Derived from	Comments
ZZS00 (1)	*ΔryhB*	BW-RI (1)	*spr-lacI-tetR* cassette derived from DH5α-ZI, *ryhB* deletion from -54 to +94
ZZS20 (1)	pZE12S	ZZS00	Wild-type *sodB*
ZZS00-W	pZE12S pZA31R	ZZS00	Same as ZZS23 (1)
ZZS00-NULL	PNULL pZA31-*lucNB* (1)	ZZS00	Negative control
ZZS00-S1	pZE12SC1 pZA31R	ZZS00	Mutant *sodB* (S1) with wild-type RyhB
ZZS00-Rt	pZE12S pZA31Rt	ZZS00	Truncated RyhB with wild-type *sodB*
ZZS00-R#	pZE12S pZA31R#	ZZS00	#: 1–11; muant RyhB in the core and flanking region.
ZZS00-H#	pZE12S pZA31RH#	ZZS00	#: 1–19; mutant RyhB in the linker region.
ZZS00-C#	pZE12SC# pZA31RC#	ZZS00	#: 1–15; complementary pairing of mutant RyhB and mutant *sodB* in the core region
ZZS0R	—	ZZS00	$P_{Ltet\text{-}O1}$ driving *ryhB* at the *ryhB* locus of the chromosome
ZZS0T	—	ZZS00	$P_{Ltet\text{-}O1}$ driving *ryhBt* at the *ryhB* locus of the chromosome
ZZS0Rq	—	ZZS0R	*hfq* mutation in ZZS0R
ZZS0Tq	—	ZZS0T	*hfq* mutation in ZZS0T

1. Levine E, Zhang Z, Kuhlman T, Hwa T (2007) Quantitative characteristics of gene regulation by small RNA. *PLoS Biol* 5:e229.

Table S2. Bacterial plasmids used in this study

Plasmid	Genotype	Derived from	Comments
pNULL (1)	*pNULL;gfpmut3b*	pZE12 (2)	colE1 *ori*, Amp marker promoter-less *gfpmut3b*
pZA31-*lucNB* (1)	$p_{LTet\text{-}o1}$*:luc*	pZA31-*luc* (2)	p15A *ori*, Cm marker *luc* gene is flanked by NdeI site and BamHI site
pZE12G (1)	$P_{lac\text{-}o1}$*:gfpmut3b*	pZE12 (2)	colE1 *ori*, Amp marker $p_{Llac\text{-}o1}$*: gfpmut3b*
pZA31R (1)	$p_{LTet\text{-}o1}$*:ryhB*	pZA31-*lucNB*	Wild-type *ryhB*
pZE12S (1)	$p_{Llac\text{-}o1}$*: crsodB-gfpmut3b*	pZE12G	Control region of wild-type *sodB* fused with a GFP reporter gene
pZA31Rt	$p_{LTet\text{-}o1}$*:ryhBt*	pZA31-*lucNB*	Truncated *ryhB*
pZA31R#	#: 1–11	pZA31-*lucNB*	*ryhB* mutants r# that contain 1–3 mutations in position 32 through 56.
pZA31RH#	#: 1–19	pZA31-*lucNB*	*ryhB* mutants *rh#* that contain mutations in position 57 through 68
pZE12SC#	#: 1–15	pZE12G	*sodB* mutants *sc#* with the two positions immediately 5′ to the start codon mutated.
pZA31RC#	#: 1–15	pZA31-*lucNB*	*ryhB* mutants *rc#* with the complementary mutations of sc#.

1. Levine E, Zhang Z, Kuhlman T, Hwa T (2007) Quantitative characteristics of gene regulation by small RNA. *PLoS Biol* 5:e229.
2. Lutz R, Bujard H (1997) Independent and tight regulation of transcriptional units in *Escherichia coli* via the LacR/O, the TetR/O and AraC/I1-I2 regulatory elements. *Nucleic Acids Res* 25: 1203–1210.

Table S3. Primers used in this study

Primer	Sequence (5′ to 3′)	Comments
sc-f	ATACGCACAATAAGGCTATTGTACGTATGC	—
sc#-r	GCATATGGTAGTGCAGGTAATTCGAATGA CATXXCTACTC	#: 1–15 XX denote all 15 point substitutions at the two positions
s0-f	CCGGAATTCATACGCACAATAAGGCTA	*EcoRI* sites
s0-r	CGGGGTACCAGCATATGGTAGTGCAG	*KpnI* sites
rc#-f	GATCAGGAAGACCCTCGCGGAGAACCTGA AAGCACGACATXXCTCACATTGCTTCCAGT	#: 1–15XX denote all 15 point substitutions at the two positions
rc-r	GCGGATCCAAAAAAAAAGCCAGCACCCGGC TGGCTAAGTAATACTGGAAGCAATGTGAG	BamHI sites
r0-f	GGAATTCCATATGCGATCAGGAAGACCCTCG	NdeI sites
r0-r	CGCGGATCCAAAAAAAAAGCCAGCACCCGGC	BamHI sites
ZA31-f	CGACGTCTAAGAAACCAT	Universal sense primer for DNA sequencing
ZA31-rn	ACCGAGCGTAGCGAGTC	Anti-sense primer for *ryhB* sequencing
sq reverse	TTGGGACAACTCCAGTGAAA	Anti-sense primer for *sodB* sequencing
PtetryhB1-P1	GGGTAAATGTCCCTTTCAACATCATTGACTTTCAA ATGCGAGTCAAATGCAGTGTAGGCTGGAGCTGCTTC	Chromosomal $P_{Ltet\text{-}O1}$ *driving ryhB*
PtetryhB2-P2	GGTGGAAAAACTGGTCGTGGACGCCTGGGAACAGC GTTCATATCACGTTGGAACCTCTTACGTGCC	Chromosomal $P_{Ltet\text{-}O1}$ *driving ryhB*
PtetryhBt2-P2	TGGATAAATTGAGAACGAAAGATCAAAAAAAAAGC CAGCACCCGGCTGGCTAAGCAATGTGAGCAATGTCG TGCTTTGTGCTCAGTATCTCTATCACTG	Chromosomal $P_{Ltet\text{-}O1}$ *driving ryhBt*
RTsodB-F	GCAATGTCATTCGAATTACCTG	*sodB* real-time PCR
RTsodB-R	CTGAGCTGCGTTGTTGAATACG	*sodB* real-time PCR
RTfumA-F	CAGTAAGTGAGAGAACAATGTC	*fumA* real-time PCR
RTfumA-R	CATGAACGACGCATCATGAAAC	*fumA* real-time PCR
RTsdhD-F	ACTGTCGTGCTTTCACTTCTCG	*sdhD* real-time PCR
RTsdhD-R	TGAACACTTTGGTGAACGCAGAG	*sdhD* real-time PCR
RTsucA-F	TTGGACTCTTCTTACCTCTCTG	*sucA* real-time PCR
RTsucA-R	TTGAAGAGTAACGTGAAGCGTC	*sucA* real-time PCR
RTryhB-F	ATATGCGATCAGGAAGACCCTC	*ryhB* and *ryhB* mutant real-time PCR
RTryhB-R	AAAGCCAGCACCCGGCTGGC	*ryhB* and *ryhB* mutant real-time PCR
RTryhBt-F	ATATGAAGCACGACATTGCTCAC	*ryhB and ryhBt* real-time PCR
RTryhBt-R	AAAAGCCAGCACCCGGCTGGCTAAG	*ryhB and ryhBt* real-time PCR
RTrrsB-F	GCTTGCTTCTTTGCTGACGAGT	*rrsB* real-time PCR
RT-rrsB-R	TGAGCCGTTACCCCACCTAC	*rrsB* real-time PCR

Table S4. R-mutants containing one to three mutations in position 32–56 of the wild-type RyhB (r1–r11)

Label	mutation region on *ryhB* (32–56)
r0	**AAGCACGACATTGCTCACATTGCTT**
r1	AAGCACGACATAGCTCACATTGCTT
r2	AAGCACGACATTGGTCTCATTGCTT
r3	AAGCACGAATTTGCTAACATTGCTT
r4	AAGCAAGACACTGCTCATATTGCTT
r5	AAGCACGACATTGATCACATTGCTT
r6	AAGCACGACATTGCTGACATTGCTT
r7	AAGCACGACATTGCTCACACTGCTT
r8	AAGCACGACGTTGCGCACATTGCTT
r9	AAGCACGACATTGCTCACATTTCTT
r10	AAGCATGCCAATGCTCACATTGCTT
r11	AAGCACTACATGGCTAACATTGCTT

"r0" denotes the corresponding fragment of the wild-type RyhB. Mutation points are indicated by an underline.

Table S5. C-mutants consisting of all 15 point substitutions at the two positions 54 and 55 of *sodB* (sc1–sc15), together with the complementary mutations at the corresponding RyhB positions (rc1–rc15)

Mutation region on *sodB*		Mutation region on *ryhB*	
Label	52–60	Label	38–46
s0	**AGCAATGTC**	**r0**	**GACATTGCT**
sc1	AGCTATGTC	rc1	GACATAGCT
sc2	AGCGATGTC	rc2	GACATCGCT
sc3	AGCCATGTC	rc3	GACATGGCT
sc4	AGGAATGTC	rc4	GACATTCCT
sc5	AGGTATGTC	rc5	GACATACCT
sc6	AGGGATGTC	rc6	GACATCCCT
sc7	AGGCATGTC	rc7	GACATGCCT
sc8	AGAAATGTC	rc8	GACATTTCT
sc9	AGATATGTC	rc9	GACATATCT
sc10	AGAGATGTC	rc10	GACATCTCT
sc11	AGACATGTC	rc11	GACATGTCT
sc12	AGTAATGTC	rc12	GACATTACT
sc13	AGTTATGTC	rc13	GACATAACT
sc14	AGTGATGTC	rc14	GACATCACT
sc15	AGTCATGTC	rc15	GACATGACT

"r0" and "s0" denote the corresponding fragments of the wild-type RyhB and *sodB*, respectively. Mutation points are indicated by an underline.

Table S6. H-mutants were generated by varying the 12 bases at positions 57–68 of RyhB (rh1–rh19)

Label	Mutation region on *ryhB* (57–68)
r0	**CCAGTATTACTT**
rh1	GATGTAATACAT
rh2	GCTGTTTTACAT
rh3	CCAGTATTTCTT
rh4	CAAGCATTGCGC
rh5	CCAGTAGTTATT
rh6	CATTTAATACTA
rh7	GCTGTGTTAATT
rh8	CCTGTCGGCGTT
rh9	CGAGCAGCGTTT
rh10	CTAGTAGTACTT
rh11	CAGTTATTCCTG
rh12	GCGGTATTCCTG
rh13	CCGTTACTACTA
rh14	ACAGCCTTCCTT
rh15	CCGGTATTACAT
rh16	CACGACATAGTT
rh17	CCAGTATTACAT
rh18	GCAGTATTACTT
rh19	ACGTTATTACTT

"r0" denotes the corresponding fragment of the wild-type RyhB. Mutation points are indicated by an underline.

Table S7. Measurement of *sodB-gfp* expression and calculation of "fold-repression"

	sodB-gfp Expression (RFU/OD/hr) [IPTG] = 1 mM				
Interaction pair	[aTc] = 0		[aTc] = 10 ng/mL		Fold-repression
W	1.3E+06	±2.0E+05	1.6E+05	±5.0E+04	8.5 ± 3.2
S1	1.3E+06	±5.3E+05	1.5E+06	±4.0E+05	0.9 ± 0.2
C1	1.5E+06	±3.0E+05	1.6E+05	±3.0E+04	9.4 ± 0.3
C2	1.6E+06	±2.0E+05	2.4E+05	±1.0E+05	6.9 ± 0.3
C3	1.2E+06	±1.0E+05	1.1E+05	±4.4E+04	13.5 ± 4.7
C4	6.1E+05	±5.0E+04	6.9E+05	±1.3E+05	0.9 ± 0.1
C5	1.0E+05	±1.2E+04	6.8E+04	±1.1E+04	1.5 ± 0.1
C6	2.9E+05	±8.0E+04	4.6E+04	±1.7E+04	6.4 ± 0.9
C7	1.2E+06	±0	1.5E+06	±0	0.8 ± 0
C8	1.4E+06	±4.0E+05	6.9E+05	±2.0E+05	2.1 ± 0.1
C9	1.4E+06	±0	3.3E+05	±1.0E+04	4.2 ± 0.2
C10	1.3E+06	±2.0E+05	9.7E+04	±2.3E+04	14.1 ± 1.6
C11	1.6E+06	±3.0E+05	3.3E+05	±1.5E+05	5.5 ± 1.6
C12	1.6E+06	±1.0E+05	5.4E+05	±6.0E+04	2.9 ± 0.1
C13	9.5E+05	±1.5E+05	5.5E+05	±7.0E+04	1.7 ± 0
C14	3.7E+05	±0	3.3E+05	±3.0E+04	1.1 ± 0.1
C15	1.3E+06	±3.0E+05	1.6E+05	±3.0E+04	8.2 ± 1.0
R1	1.2E+06	±2.2E+05	1.4E+06	±2.0E+05	0.9 ± 0.1
R2	1.1E+06	±0	1.6E+06	±1.0E+05	0.7 ± 0
R3	1.2E+06	±0	1.2E+06	±0	1.0 ± 0
R4	1.2E+06	±2.0E+05	9.9E+05	±1.6E+05	1.2 ± 0.1
R5	1.4E+06	±1.0E+05	1.5E+06	±1.0E+05	1.0 ± 0
R6	1.3E+06	±2.0E+05	6.4E+04	±5.0E+03	20.3 ± 2.0
R7	1.2E+06	±1.0E+05	1.2E+05	±0	9.9 ± 0.7
R8	1.3E+06	±1.0E+05	9.6E+05	±5.0E+04	1.4 ± 0.1
R9	1.2E+06	±3.0E+05	7.9E+04	±3.1E+04	15.4 ± 2.8
R10	1.5E+06	±1.0E+05	1.9E+06	±1.0E+05	0.8 ± 0.1
R11	1.6E+06	±0	1.6E+06	±0	1.0 ± 0
H1	1.1E+06	±8.0E+04	1.1E+05	1.5E+04	10.0 ± 0.5
H2	8.3E+05	±9.0E+04	1.3E+05	±2.0E+04	6.3 ± 0
H3	1.4E+06	±0	1.5E+05	±1.0E+04	9.5 ± 0.7
H4	8.2E+05	±3.0E+04	2.0E+05	±1.0E+04	4.0 ± 0.2
H5	8.8E+05	±1.0E+05	6.5E+04	±1.3E+04	13.9 ± 1.3
H6	1.3E+06	±2.0E+05	1.2E+05	±7.0E+04	13.1 ± 5.1
H7	9.5E+05	±8.0E+04	1.8E+05	±1.0E+04	5.3 ± 0.2
H8	1.4E+06	±2.0E+05	3.9E+05	±4.0E+04	3.6 ± 0.1
H9	9.7E+05	±1.0E+05	3.5E+05	±4.0E+04	2.7 ± 0.1
H10	1.2E+06	±2.6E+05	7.4E+04	±3.6E+04	16.8 ± 5.7
H11	1.0E+06	±1.0E+05	7.8E+04	±1.3E+04	13.7 ± 2.7
H12	1.1E+06	±2.0E+05	8.4E+05	±5.0E+04	1.3 ± 0.2
H13	1.3E+06	±1.0E+05	2.9E+05	±7.0E+04	4.5 ± 0.8
H14	9.2E+05	±3.8E+05	1.7E+05	±8.1E+04	5.9 ± 0.7
H15	1.2E+06	±0	5.4E+05	±4.0E+04	2.2 ± 0.1
H16	8.7E+05	±3.3E+05	1.0E+05	±4.0E+04	8.9 ± 0.5
H17	1.3E+06	±1.0E+05	1.3E+05	±2.0E+04	9.9 ± 0.8
H18	1.2E+06	±2.0E+05	8.0E+04	±3.0E+04	16.5 ± 4.0
H19	1.2E+06	±1.0E+05	5.7E+04	±1.4E+04	22.0 ± 5.2

Error bars were calculated according to two or more repeated measurements.

Table S8. Quantitative real-time PCR results of expression levels of plasmid-harboring *ryhB* and *ryhB* mutants

Strain (ZZS00-)	Relative abundance of sRNA [aTc] = 10 ng/mL
W	1.0
R6	0.5
R8	0.4
R11	0.0001
C3	1.2
C8	3.2
H11	3.4
H12	1.9
H15	1.5
H19	1.1

Abundances of RyhB (W) and RyhB mutants (R-, C-, and H-mutants) were determined by quantitative real-time PCR in strains induced with 10 ng/mL aTc, with the level of 16S RNA as internal control; detailed description in *SI Materials and Methods*. Here we show the RNA abundances relative to the wild-type RyhB level in strain ZZS00-W.

Table S9. Ensemble free energy predicted for each interaction pair: free energy of RyhB-*sodB* duplex (E_{duplex}), self-binding free energy for RyhB (E_{RyhB}) and control region of *sodB* (E_{sodB}), and free energy of duplex formation (ΔE)

	Energy values (kcal/mol)			
Interaction pair	E_{RyhB}	E_{sodB}	E_{duplex}	ΔE
W	−26.5	−17.32	−54.58	−10.76
C1	−26.17	−17.78	−54.97	−11.02
C2	−26.36	−17.87	−56.37	−12.14
C3	−27.53	−17.24	−56.97	−12.2
C4	−25.85	−21.09	−54.78	−7.84
C5	−25.86	−24.01	−54.98	−5.11
C6	−25.86	−21.86	−57.17	−9.45
C7	−26.49	−20.73	−56.97	−9.75
C8	−25.89	−17.36	−52.38	−9.13
C9	−25.88	−17.8	−52.98	−9.3
C10	−25.89	−17.38	−55.08	−11.81
C11	−27.31	−17.28	−54.88	−10.29
C12	−25.86	−18.86	−52.58	−7.86
C13	−25.86	−17.82	−52.59	−8.91
C14	−25.86	−18.96	−54.88	−10.06
C15	−26.46	−17.3	−54.9	−11.14
R1	−26.17	−17.32	−50.69	−7.2
R2	−28.48	−17.32	−51.12	−5.32
R3	−26.35	−17.32	−52.95	−9.28
R4	−27.52	−17.32	−50.76	−5.92
R5	−25.9	−17.32	−51.88	−8.66
R6	−27.04	−17.32	−55.76	−11.4
R7	−26.51	−17.32	−55.56	−11.73
R8	−27	−17.32	−54.72	−10.4
R9	−27.5	−17.32	−55.58	−10.76
R10	−28.29	−17.32	−52.61	−7
R11	−29.76	−17.32	−50.45	−3.37
H1	−26.98	−17.32	−53.85	−9.55
H2	−26.46	−17.32	−53.4	−9.62
H3	−28.42	−17.32	−53.76	−8.02
H4	−29.78	−17.32	−55.79	−8.69
H5	−26.59	−17.32	−54.4	−10.49
H6	−26.82	−17.32	−53.66	−9.52
H7	−28.82	−17.32	−56.68	−10.54
H8	−31.88	−17.32	−55.7	−6.5
H9	−30.82	−17.32	−54.69	−6.55
H10	−26.32	−17.32	−54.07	−10.43
H11	−30.57	−17.32	−54.86	−6.97
H12	−32.35	−17.32	−56.27	−6.6
H13	−27.18	−17.32	−53.76	−9.26
H14	−28.38	−17.32	−55.58	−9.88
H15	−26.8	−17.32	−55.39	−11.27
H16	−26.45	−17.32	−52.57	−8.8
H17	−26.44	−17.32	−54.47	−10.71
H18	−26.83	−17.32	−54.06	−9.91
H19	−25.41	−17.32	−54.58	−11.85

See *SI Materials and Methods*.

Table S10. Expression levels of *sodB-gfp* in strains ZZS00-W and ZZS00-C1 through ZZS00-C15 in the absence of RyhB expression (no aTc), together with the energy cost (E^*_{sodB}) of opening both the interaction core region (52–60) and the Hfq-binding region (29–44) of *sodB*

Interaction pair	*sodB-gfp* expression (RFU/OD/hr) [IPTG] = 3 mM	E^*_{sodB} (kcal/mol)
W	1.9E+06	6.11
C1	2.1E+06	6.57
C2	1.4E+06	6.66
C3	2.0E+06	6.03
C4	5.2E+05	9.88
C5	1.2E+05	12.8
C6	2.8E+05	10.65
C7	3.7E+05	9.52
C8	2.0E+06	6.15
C9	1.9E+06	6.59
C10	1.4E+06	6.17
C11	1.6E+06	6.07
C12	1.2E+06	7.65
C13	1.3E+06	6.61
C14	6.4E+05	7.75
C15	1.2E+06	6.09

Table S11. Best-fit parameters of the data in Fig. 2*A* (main text)

Strain	λ (nM/min)
W	1.85 ± 0.48
C3	0.67 ± 0.22
C8	11.69 ± 2.68
C9	3.80 ± 0.94
C10	0.78 ± 0.28
C11	1.59 ± 0.43
C15	1.92 ± 0.48

Best-fit value for α_s is 21.30 ± 3.24 nM/min. Detailed description in *SI Materials and Methods*.

Table S12. AU content of the Hfq-binding region of RyhB (position 57–68) and the energy cost (ΔE_{linker}) of keeping this region open

RyhB	No. AU	ΔE_{linker} (kcal/mol)
RyhB-r0	8	1.48
RyhB-rh1	9	1.94
RyhB-rh2	8	1.42
RyhB-rh3	8	3.4
RyhB-rh4	5	4.69
RyhB-rh5	8	1.57
RyhB-rh6	10	1.73
RyhB-rh7	8	3.78
RyhB-rh8	4	6.86
RyhB-rh9	5	5.8
RyhB-rh10	8	1.3
RyhB-rh11	7	5.4
RyhB-rh12	5	7.17
RyhB-rh13	7	2.09
RyhB-rh14	6	3.34
RyhB-rh15	7	1.78
RyhB-rh16	7	1.43
RyhB-rh17	8	1.42
RyhB-rh18	8	1.79
RyhB-rh19	9	0.37

Definition and calculation of ΔE_{linker} values in *SI Materials and Methods*.

Table S13. Quantitative real-time PCR results for expression of chromosomal encoded *ryhB* and *ryhBt* in the *hfq*$^+$ (ZZS0R and ZZS0T, respectively) and *hfq*$^-$ (ZZS0Rq and ZZS0Tq, respectively) strains induced with 10 ng/mL aTc

Strain	Relative abundance of sRNA [aTc] = 10 ng/mL
ZZS0R	0.9
ZZS0T	1.2
ZZS0Rq	0.2
ZZS0Tq	1.0

RNA abundances were normalized to the level of 16S RNA (encoded by *rrsB*), which was chosen as an internal control. Detailed description in *SI Materials and Methods*.

Table S14. Quantitative real-time PCR results for effect of chromosomal encoded *ryhB* and *ryhBt* on expression of various chromosomal targets (*sodB*, *fumA*, *sdhD*, and *sucA*) in *hfq*$^+$ strains

		Relative abundance			
Strain	Condition	*sodB*	*fumA*	*sdhD*	*sucA*
ZZS0R	[aTc] = 0	1.1	1.2	1.2	1.2
	[aTc] = 10 ng/mL	0.2	0.4	0.4	1.2
ZZS0T	[aTc] = 0	1.0	1.0	1.0	1.0
	[aTc] = 10 ng/mL	0.1	0.1	0.2	1.0

RNA abundances were normalized to the level of 16S RNA (encoded by *rrsB*), which was chosen as an internal control. Detailed description in *SI Materials and Methods*.

Table S15. Quantitative real-time PCR results for effect of chromosomal encoded *ryhB* and *ryhBt* on expression of various chromosomal targets (*sodB*, *fumA*, *sdhD*, and *sucA*) in *hfq*$^{-}$ strains

Strain	Conditions	Relative abundance			
		sodB	*fumA*	*sdhD*	*sucA*
ZZS0Rq	[aTc] = 0	1.1	1.1	1.0	0.9
	[aTc] = 10 ng/mL	1.0	1.3	1.1	1.3
ZZS0Tq	[aTc] = 0	1.2	1.2	1.1	0.9
	[aTc] = 10 ng/mL	0.1	0.2	0.2	1.0

RNA abundances were normalized to the level of 16S RNA (encoded by *rrsB*), which was chosen as an internal control. Detailed description in *SI Materials and Methods*.